Variability of currents and mixing processes during the onset of the Equatorial Cold Tongue in the Atlantic

Bachelor Thesis in the subject Physik des Erdsystems

Faculty of Mathematics and Natural Sciences

Christian-Albrechts-University of Kiel

Referee: Dr. Marcus Dengler

Co-Referee: Prof. Dr. Peter Brandt

submitted by

Sebastian Milinski

Kiel July 2012

Contents

Zusammenfassung

Der Wärmeinhalt der Ozeane ist von zentraler Bedeutung für die großskalige Zirkulation in den Ozeanen sowie für den Ozean-Atmosphären-Austausch und hat damit auch unmittelbaren Einfluss auf unser Klima. Die Verbindung zwischen dem Ozean und der Atmosphäre erfolgt über die in sich weitestgehend homogene Deckschicht der Ozeane.
Entscheidend für den Wärmeinhalt der Deckschicht sind Prozesse, die eine Verbindung zwischen der Deckschicht und der Atmosphäre sowie der Deckschicht und den tiefer liegenden Wassermassen herstellen. Im Rahmen dieser Arbeit werden Vermischungsprozesse in sowie unter der Deckschicht und Ihre zeitliche Variabilität näher untersucht.
Messungen im Äquatorialen Ostatlantik im Mai-Juni 2011 geben Hinweise auf turbulente Vermischungsprozesse, die auch deutlich unter der Deckschicht stattfinden und damit eine Verbindung zwischen der Deckschicht und den tiefer liegenden Wassermassen darstellen. Diese Prozesse weisen einen ausgeprägten Tagesgang mit einem Maximum in der zweiten Nachthälfte bis weit in den Vormittag hinein auf. Diese Maxima treten stets in Verbindung mit schwacher vertikaler Schichtung sowie starker vertikaler Geschwindigkeitsscherung in der Wassersäule auf. Neben dem Tagesgang wurde eine überlagerte Periodizität von 11 Tagen gefunden. Diese führt dazu, dass an einigen Tagen keine turbulente Vermischung unterhalb der Deckschicht nachgewiesen werden konnte während einige Tage später turbulente Vermischungsprozesse bis zu 30 Meter unter der Deckschicht beobachtet wurden.

Abstract

The heat content of the surface water masses is important for the circulation of the oceans and the atmosphere. The surface layer serves as a medium for the ocean-atmosphere exchange and thereby significantly affects the dynamics of our climate. Despite this, many of the mechanisms that allow exchange between the surface layer and the ocean interior are still elusive.

Measurements of the turbulent dissipation rate of kinetic energy in May and June 2011 in the Atlantic Cold Tongue region depict mixing events that extend below the surface mixed layer. These mixing processes show a distinct diurnal cycle with a nighttime maximum, which is preserved until some hours after sunset. These deep mixing events occur when the stratification is weak and high vertical shear is present.

The diurnal cycle is superimposed on a low-frequent variation of the turbulent dissipation rate of kinetic energy. Due to this low frequent cycle with a period of 11 days, the increased mixing events below the mixed layer vanish completely during some days while they extend 30 meters below the mixed layer depth on other days.

1 Introduction

1.1 Background conditions

The Tropical Atlantic Ocean shows a strong seasonal variability of the sea surface temperature (SST). The westerly winds at the equator drive meridional Ekman Transport leading to upwelling of cold water masses at the equator generating the Equatorial Cold Tongue, which reaches its minimum surface temperature in August. Jouanno et al. found the vertical turbulent exchanges to be of major importance for the surface cooling. The intraseasonal variability of the South Equatorial Current is presumed to have an impact on the seasonal cycle of the Equatorial Cold Tongue by modulating the current shear and thus changing the vertical turbulent fluxes (Jouanno et al. 2011).
Below the surface there is a strong eastward flowing current with maximum velocities exceeding 1 m/s. The core depth is deepest in the west and rises to about 50m in the east. The driving force of this Equatorial Under Current (EUC) is assumed to be a zonal pressure gradient caused by the surface winds (Pedlosky 1996). The water masses accumulated in the west create a pressure gradient which is balanced by the eastward flowing EUC.

1.2 Mixing in the Cold Tongue region

The Atlantic Cold Tongue is among the regions in the ocean with the largest heat transport from the atmosphere into the ocean. The mechanisms driving the surface cooling are still under investigation, but vertical turbulent exchanges are suspected to have a major influence on the development of the Atlantic Cold Tongue (Jouanno et al. 2011). The strong vertical shear of the currents near the EUC presents favorable conditions for shear instabilities that create turbulent mixing. Mixing works through molecular diffusion which is greatly enhanced by turbulences enlarging the surface over which molecular diffusion can act and increasing the gradients.
The features of the Atlantic Cold Tongue are similar to the Pacific Cold Tongue. In 1984 several expeditions have been conducted in the Equatorial Pacific, during which a considerable number of vertical profiles of the turbulent kinetic energy dissipation rate (ε) have been measured (Moum et al. 1992). The turbulent kinetic energy dissipation rate describes the dissipation of kinetic energy into molecular movement. An interesting feature which was not anticipated is a nighttime enhancement of ε during a cruise in November 1984 in the equatorial Pacific (Gregg et al. 1985). This diurnal cycle was present in the mixed layer

as well as in the stratified layer below the mixed layer depth (MLD). It is assumed that strong vertical shear of the currents supports turbulent mixing. As a mechanism for the deep diurnal cycle - the enhanced mixing below the surface mixed layer - internal waves were suggested that trigger turbulent mixing in the strong shear region.

In the late 1980s several attempts have been made to further analyze the characteristics of the deep diurnal cycle and the background conditions that lead to enhanced turbulent mixing. Moored temperature observations revealed that the averaged temperature variance during nighttime was three times higher than during daytime (McPhaden and Peters 1992). Towed thermistor-chain observations along the equator in April 1987 supported the assumption that vigorous mixing events occur especially during nighttime. These events seem to have a small extent in space and time (Hebert et al. 1992).

In 1989 the presence of two distinct mixing regimes was described (Moum et al. 1989). The surface layer is characterized by a diurnal cycle of the surface buoyancy flux and associated mixing. Below the base of the surface mixed layer, a more distinct day-night cycle was observed. During nighttime turbulent bursts with a duration of 2-3 hours have been observed that contribute to the variability of mixing rates. These bursts are believed to be connected to internal wave breaking events.

In 1995 Lien et al. assumed a close connection between the rapid sea surface temperature increase during the onset of an El Niño event and the decrease of vertical heta flux (Lien et al. 1995). This would add another mechanism to the observed SST increase thus offering a more complete explanation of the complex mechanisms. The lateral advection of water masses was not sufficient to explain the observed phenomenon to the full extent.

Richards et al. recently investigated the effects of the El Niño Southern Oscillation on the levels of mixing in the western equatorial Pacific (Richards et al. 2012). They found that the levels of mixing in the surface mixed layer and below were strongly influenced by small scale vertical flow features. During perennial observations the levels of mixing were significantly higher during La Niña events.

In 2009 Moum et. al studied the influence of tropical instability waves on subsurface mixing and their impact on surface cooling (Moum et al. 2009). Tropical instability waves are a meridional deflection of the boundary between cold an warm surface water masses near the equator. These westward-propagating waves have a period of about 30 days. The meridional displacement of the surface water masses leads to an intensified vertical shear above the EUC. In the presence of a tropical instability wave measurements of the dissipation rate of turbulent kinetic energy showed a distinct increase as opposed to measurements in the absence of a tropical instability wave. Further increasing the shear above the

EUC the tropical instability wave shifts the conditions towards instability which leads to turbulent mixing processes.

1.3 Mixing in the Atlantic Cold Tongue region in 2011

In the present study continuous glider-based measurements of the turbulent dissipation rate of kinetic energy (ε) that have been conducted in May-June 2011 in the Atlantic Cold Tongue region are used. These measurements are analyzed for periodic variations of ε. A thorough description of the variability of these mixing processes and the associated background conditions has been carried out.

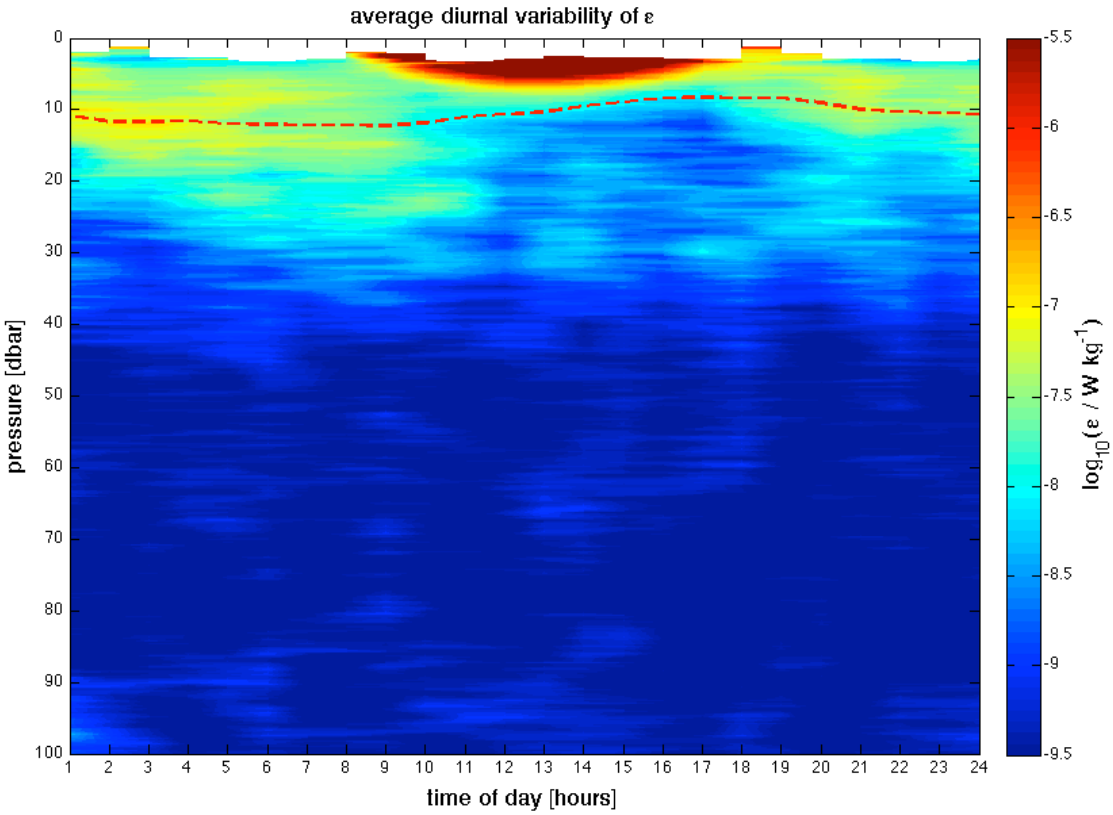

***Figure 1-1**, the diurnal variation of the turbulent dissipation rate of kinetic energy ε during a glider deployment at 0° N 10° W from June 13th to June 29th, values of ε have been calculated as one hour bins of mean values from the whole glider deployment. The red dashed line indicates the mixed layer depth.*

In addition to the glider-based measurements that include temperature and salinity a velocity dataset from a moored acoustic doppler current profiler (ADCP) is used. A comparison of the stratification and shear variability both in space and time will be used to deduce the conditions that lead to the observed turbulence.

2 Data and Methods

2.1 Data

2.1.1 Glider measurements

The data sets for the turbulent dissipation rate of kinetic energy have been collected during two glider deployments at the equator at 10°W. A glider is an oceanographic sensor platform without any propulsion system. It can adjust its diving depth by changing its density. Course corrections can be done by a rudder similar to that of an airplane. The glider is constantly profiling the water column and delivers a time series data set. A microstructure probe has been mounted on the glider to measure the fine-structure of current shear as well as pressure, salinity and temperature. The glider has been deployed two times at the equator near 10° W. The first deployment was on 26th of May 2011 and it was recovered on 12th of June 2011. During this deployment the glider was circling around a mooring (compare figure 2-2 for position). The second deployment was on June 13th, the glider was recovered on the 9th of July. The data that has been provided for this study was on a 0,25 dbar pressure grid and a not uniformly spaced time grid with an approximate spacing of one hour.

***Figure 2-1**, a microstructure probe mounted on a glider, Copyright 2012: Algot Kristoffer Peterson*

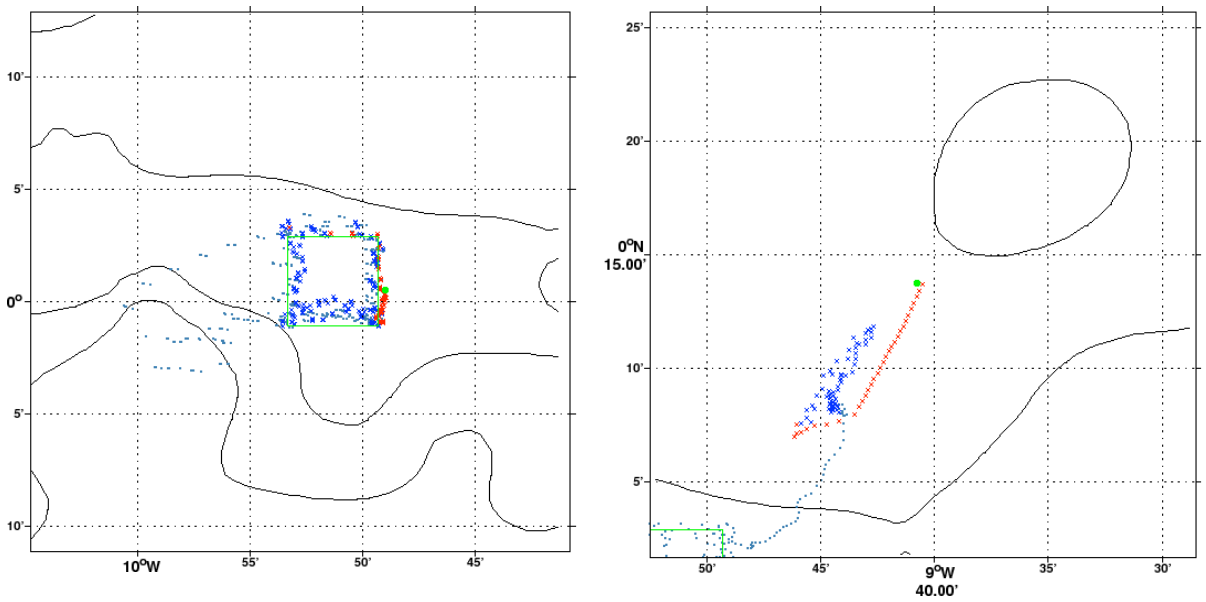

***Figure 2-2**, left: track of the first glider deployment (05/26/11-06/12/11), right: track of the second glider deployment (06/13/11-07/09/11)*

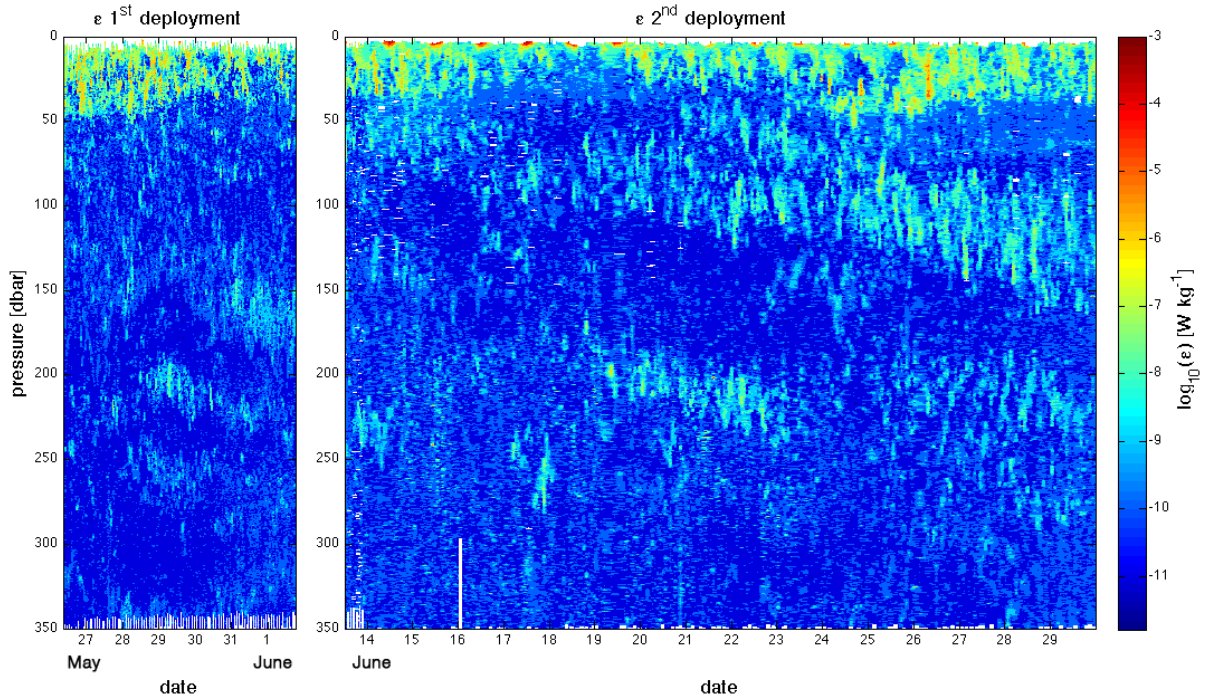

Figure 2-3: *turbulent kinetic energy dissipation rate from the 1st and 2nd glider deployment*

The turbulent kinetic energy dissipation rate as depicted in figure 2-3 has been derived from the microstructure measurements. Due to technical problems there were only 6 days of data recorded during the first deployment. This limits some of the methods that have been used to analyze the data. In this study both data sets were analyzed the same way and revealed similar processes. For improving clarity the presentation of the results will be based on the data from the second deployment.

2.1.2 Mooring

In addition to the glider measurements, velocity data from a moored acoustic doppler current profiler (ADCP) has been provided. The mooring, located near 0°N 10°W is a part of the PIRATA program (Prediction and Research Moored Array in the Atlantic) which consists of several moored observatories in the Atlantic. The velocities have been determined by an acoustic method. A sound signal is transmitted and the reflection is recorded. By using the doppler effect the frequency shift of the reflected signal yields the velocity of the reflector - mostly some particle moving with the currents. The velocity data has been provided on a 2 dbar pressure grid from 0 dbar to 170 dbar. The dataset begins in October 2010 and ends in November 2011 with a temporal resolution of one hour. The moored ADCP did not reach up to the surface to avoid the influence of wind and waves on the alignment of the mooring. Continuous data of ocean and surface parameters is constantly

being collected by a number of PIRATA moorings with a surface buoy. The subsurface temperature data of the mooring at 0°N 10°W and the temperature data gathered by the glider has is used in this study to determine the mixed layer depth.

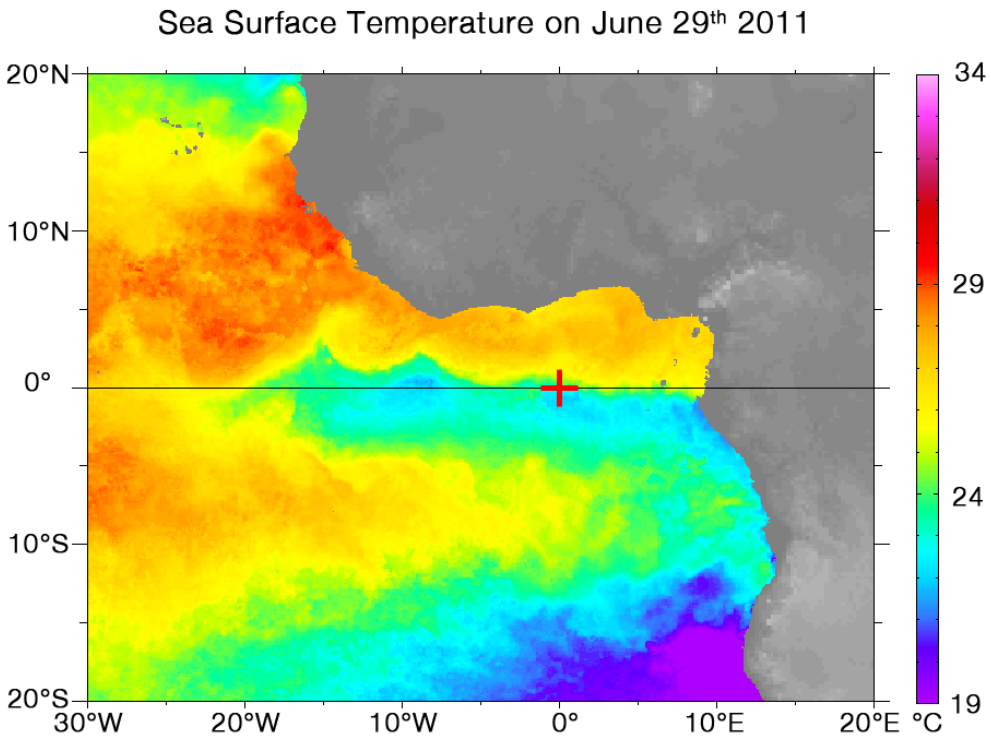

Figure 2-4, *sea surface temperature from satellite measurements[1] on the 29th of June 2011, PIRATA mooring locations(red), all glider measurements within 0.3° distance of the mooring location*

2.2 Methods

2.2.1 Mixed layer depth

The depth of the lower boundary of the well-mixed surface layer, the *mixed layer depth*, has been calculated from the glider measurements and from the PIRATA mooring. The mixed layer depth has been defined as the depth where the temperature is 0.2°C lower than the mean temperature value from 3-6 meters of depth.

2.2.2 Time-series analysis, diurnal cycle

One of the main objectives of this study was to examine whether a diurnal cycle similar to the observed diurnal cycle in the Pacific is present in the data. Therefore the time series of the glider deployment was analyzed by creating an averaged profile of the upper 100 meters of the water column for each hour of the day. (figure 1-1)

1 AMSR-E data are produced by Remote Sensing Systems and sponsored by the NASA Earth Science MEaSUREs DISCOVER Project and the AMSR-E Science Team. Data are available at www.remss.com.

Based on figure 1-1 and earlier studies (Peters et al. 1988; Gregg et al. 1985) the day was divided into four sections of equal length to calculate mean profiles for different parameters. (2 am to 8 am, 8 am to 2 pm, 2 pm to 8 pm, 8 pm to 2 am, all times in UTC). The mean profiles for ε, S^2 (vertical shear), N^2 (stratification) and temperature were derived from the data.

2.2.3 Properties of the water column

As an indicator for the stability of the stratification the buoyancy frequency (Brunt-Väisälä frequency) was calculated. It describes the frequency of a parcel of water, which is oscillating after being vertically displaced from its location in the water column. Depending on the density of the parcel and the surrounding water masses, the parcel will oscillate with a certain frequency around its original position. In a highly stratified fluid, the buoyancy frequency (N) will be higher than in a less stratified fluid.

$$N = \sqrt{-\frac{g}{\rho} * \frac{d\rho}{dz}}$$

g: local acceleration of gravity

ρ: potential density, depending on temperature and salinity

z: geometric height

If the gradient of temperature and salinity is near the maximum sensor resolution, it will become necessary to calculate the buoyancy frequency over a larger interval. The interval for the first deployment was set to 12 meters and for the second deployment to 4 meters. Because of the small vertical gradient in the mixed layer it was necessary to exclude the mixed layer from the calculation of the stratification.

The current shear has been derived from the ADCP velocity data. Both zonal and meridional shear have been calculated as the gradient of a linear fit over 12 meter intervals (4 meter intervals) for the first (second) deployment. The total shear S^2 was calculated as the sum of the components squared:

$$S^2 = \frac{du}{dz}^2 + \frac{dv}{dz}^2$$

Shear and stratification are the most important influences when it comes to mixing processes due to turbulent instabilities of currents. The basic theory is that two bodies of a fluid with different density and moving at a different speed might develop instabilities at their boundary. Initial wavelike features will form at the interface between the fluids. If there is a high stratification, the waves will not grow any further whereas a high shear will support initial waves. If the waves grow further, they will ultimately break which leads to turbulent

mixing. The probability that turbulent mixing occurs can be described by the Richardson number that compares stratification and shear.

$$Ri = \frac{N^2}{S^2}$$

If Ri < 0.25 turbulent mixing might occur (Thorpe 1973). This does not mean that mixing will inherently occur but the background conditions are favorable. For the purpose of better visualization the Froude number will be used.

$$Fr = \frac{1}{Ri} = \frac{S^2}{N^2}$$

If Fr > 4 turbulent mixing might occur.

2.2.4 Spectral analysis

The presence of a diurnal cycle leads to the assumption that a higher variance should be observable in distinct frequency bands. The power spectral density function has been estimated by a Fourier transformation of the autocovariance function (Dengler 1995).

$$F_{(\lambda)} = C_0 + 2 * \sum_{t=1}^{N-1} C_t * \cos(2\pi\lambda t)$$

$$C_t = \frac{1}{N} \sum_{t=1}^{N-1} x_n * x_{n+t}$$

$F_{(\lambda)}$: spectral density function
C_t : autovariance function
x_n : sensor reading
N : number of sensor readings

Welch's method was used in order to minimize the noise in the analyzed time series: the time series is divided into several sections that have a 50% overlap. For each section a periodogram is calculated based on a chi-square distribution. The power spectral density function is calculated as the mean of all periodograms. The Power Spectrum Density has been plotted conserving the variance.

The spectral analysis requires a uniformly spaced time-series. The measurements of ε from the glider deployment have been moved to a uniformly spaced time-grid without changing the measured values. The method of interpolation has not been used by intention because there are no well-established methods for doing spectral analysis of time series data of ε.

3 Results

3.1 Temporal and vertical structure

The temporal and vertical distribution of turbulent kinetic energy dissipation rate, stratification, total shear and Froude number is depicted in figure 3-1 for the second glider deployment. The mixed layer depth has been calculated from temperature data from the glider.

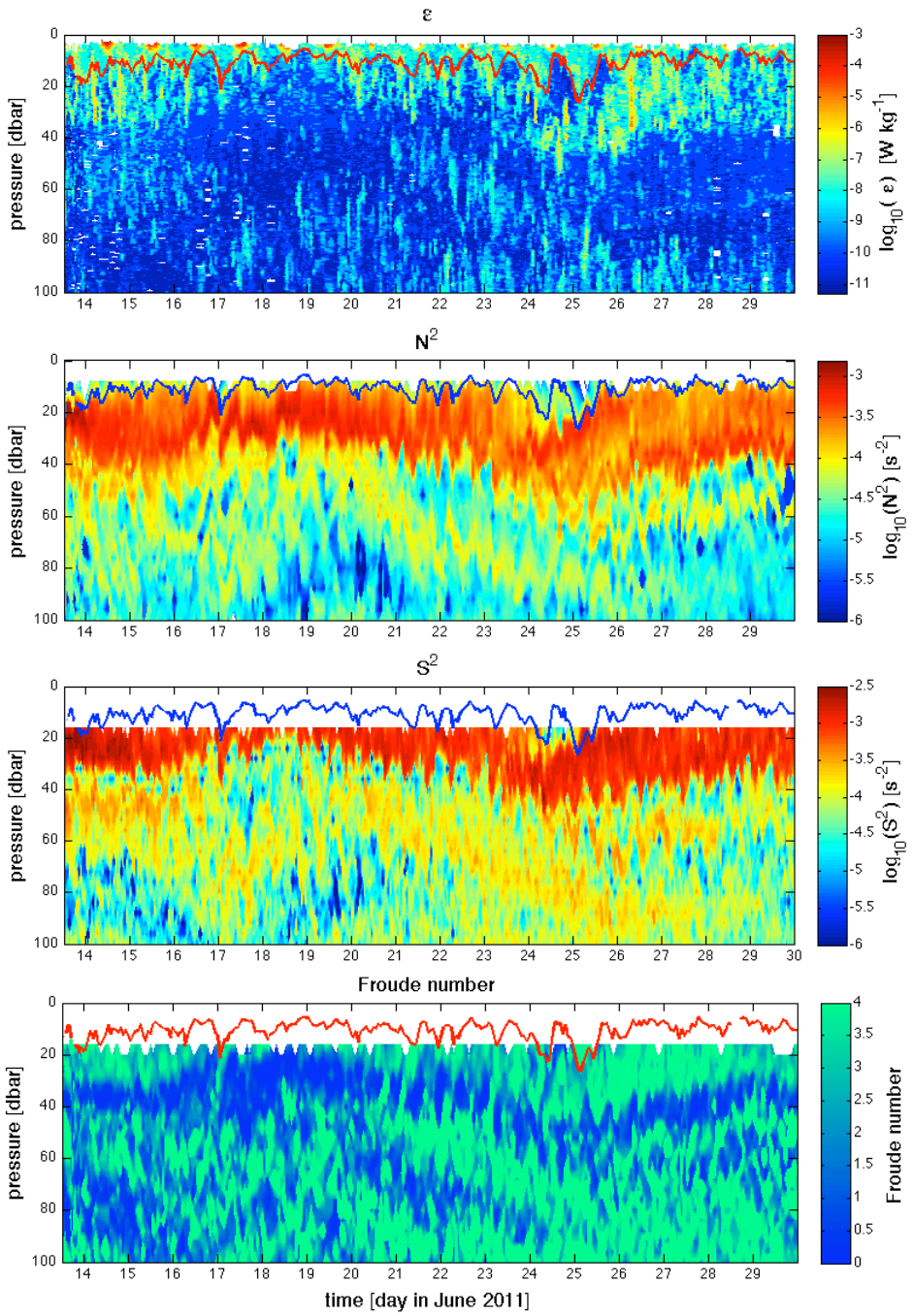

Figure 3-1: *temporal and vertical distribution of (from top to bottom): turbulent kinetic energy dissipation rate ε, buoyancy frequency N^2, total shear S^2, Froude number; the solid red/blue line marks the mixed layer depth; all data measured during the second glider deployment (06/13/11-06/29/11), date ticks mark 00:00 UTC*

The turbulent kinetic energy dissipation rate shows an increase at the surface each day at noon. This daily maximum close to the surface is connected to the diurnal variation of the surface buoyancy flux. The mixed layer is characterized by high rates of mixing at all times with a minimum during the night. Below the mixed layer depth there are bursts of ε that reach down to ~50 meters which is about 30 meters below the mixed layer depth. These deep reaching bursts reach their maximum values shortly after midnight and seem to vanish completely after noon. In addition to a diurnal cycle there is a periodicity of ~11 days both in strength and depth of these bursts. Maximum values can be found on the 14th and 26th of June while there are no noticeable turbulent events below the mixed layer from the 17th to the 19th of June. Another prominent feature are elevated rates of ε far below the mixed layer depth with no connection to the regions of high levels of ε directly below the mixed layer depth. One of these features starts on June 21st at about 50 meters depth and propagates further downwards during the next few days. Although there seems to be no direct connection to the turbulent events directly below the mixed layer depth, this feature still shows a distinct cycle with a periodicity of about one day while propagating downwards.

The buoyancy frequency is lowest in the surface layer where the density remains nearly constant with depth. Below the mixed layer depth, there is a layer of increased stratification, the thermocline. The diurnal cycle of the stratification is not as pronounced as for ε as there is no noticeable diurnal variation in the magnitude of the stratification, but there is a distinct diurnal cycle in the thickness of the thermocline. This layer advances to maximum depths of about 50 meters on the 15th and 26th of June. A patch slightly more stratified than the surrounding water masses starts to propagate downward from the mixed layer on June 19th.

The total shear is highly elevated directly below the mixed layer. As there was no velocity data available near the surface, the shear in the mixed layer could not be calculated. The maximum depth of high levels of shear shows a periodicity of 24 hours or less superimposed on a well pronounced periodicity of about 11 days. The maximum depth is reached on the 15th and 25th of June. On the 24th of June very low levels of shear directly below the mixed layer depth have been recorded. There is another layer with elevated levels of shear below 40 meters of depth that is not directly connected to the high shear layer below the mixed layer. This signal shows a diurnal cycle of magnitude while the depth varies with a period of about 11 days but seems to lag the low frequent depth variation of the shear layer directly below the mixed layer by one or two days.

The Froude number has been calculated as described in section 2.2.3. Because of the missing velocity data from directly below the surface it was not possible to determine the Froude number in the upper 15 meters. If the Froude number reaches values above four then turbulent mixing is likely to occur; if the Froude number is close to zero, it is very unlikely that turbulent mixing occurs. Although the Froude number reaches values above four, these values are accumulated in the highest values of the color-coding. The increments just below four have a greater relevance in this study because they give an impression on how close the conditions are to being unstable and allowing for turbulent mixing. The Froude number is close to four until some meters below the mixed layer and shows a slight diurnal cycle during some periods of the glider deployment. Starting at about 10-20 meters below the mixed layer, there is a layer where the Froude number is close to zero for the whole time. This layer is thickest from the 17th to the 20th of June. The depth of this layer varies with a period of ~11 days and reaches its maximum depth on the 26th of June. Below this layer, there are some patches where the Froude number is close to four. These patches become stronger and last longer during the second half of the deployment.

3.2 Deep diurnal cycle

The diurnal variation of ε found in figure 3-1 has been further analyzed by calculating 24 average vertical profiles from all measurements of the second deployment.

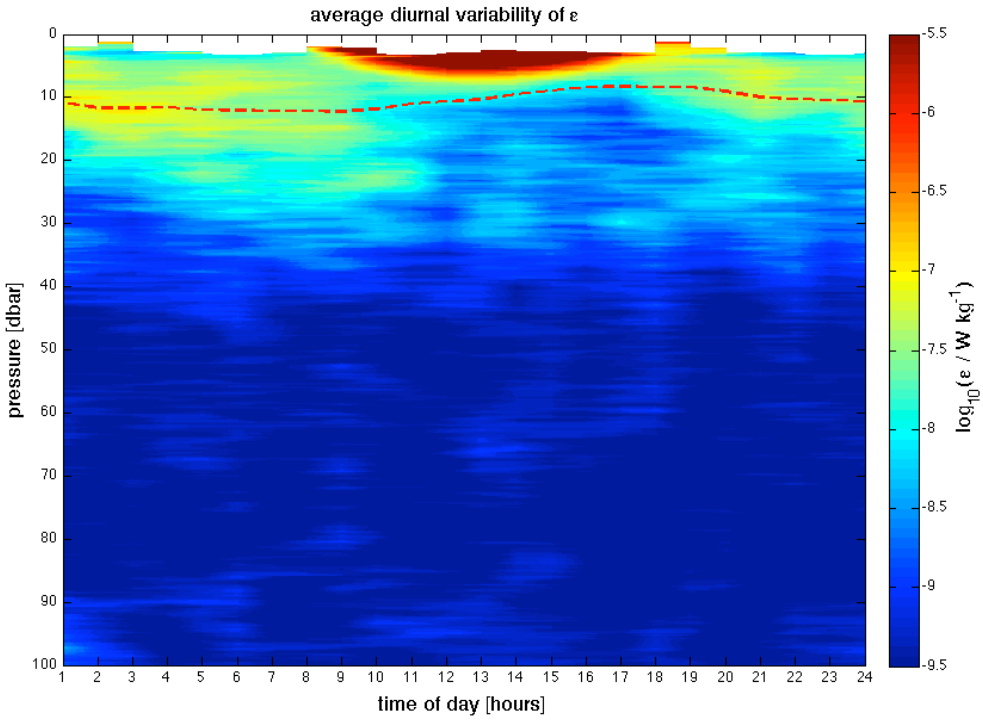

Figure 3-2: *average diurnal variability of the turbulent kinetic energy dissipation rate ε, mean pro-*

files for each hour of the day derived from the data collected during the second deployment (06/13/11-06/29/11), red dashed line: average mixed layer depth

The averaged turbulent kinetic energy dissipation rate indicates maximum levels of more than $10^{-5.5}$ W kg^{-1} at the surface during the day. This maximum is closely connected to the surface buoyancy flux. From 12:00 - 18:00 UTC the mixed layer depth clearly marks the lower boundary for elevated levels of ε. At 18:00 UTC the levels of ε about 5 meters below the mixed layer start increasing by a factor of 10^1-10^2. After 00:00 UTC the magnitude increases even further and the elevated levels of ε reach farther below the mixed layer. In the period from 02:00 - 12:00 UTC the turbulent kinetic energy dissipation rate up to 15 meters below the mixed layer has increased by a factor of 10^2-10^3 compared to the minimal values in the respective region during the rest of the day. A distinct diurnal cycle of ε has been present throughout most of the time of the second deployment.

The average diurnal variability of the stratification shows the presence of a well-stratified layer below the mixed layer throughout all of the day. The stratification decreases below 40 meters of depth. The highly stratified thermocline is centered in between 20-30 meters of depth. The magnitude of stratification and the thickness of the thermocline vary throughout the day. The highest values can be found from 12:00 - 21:00 UTC. During the night, the magnitude decreases until it reaches the lowest levels of stratification from 06:00- 12:00 UTC.

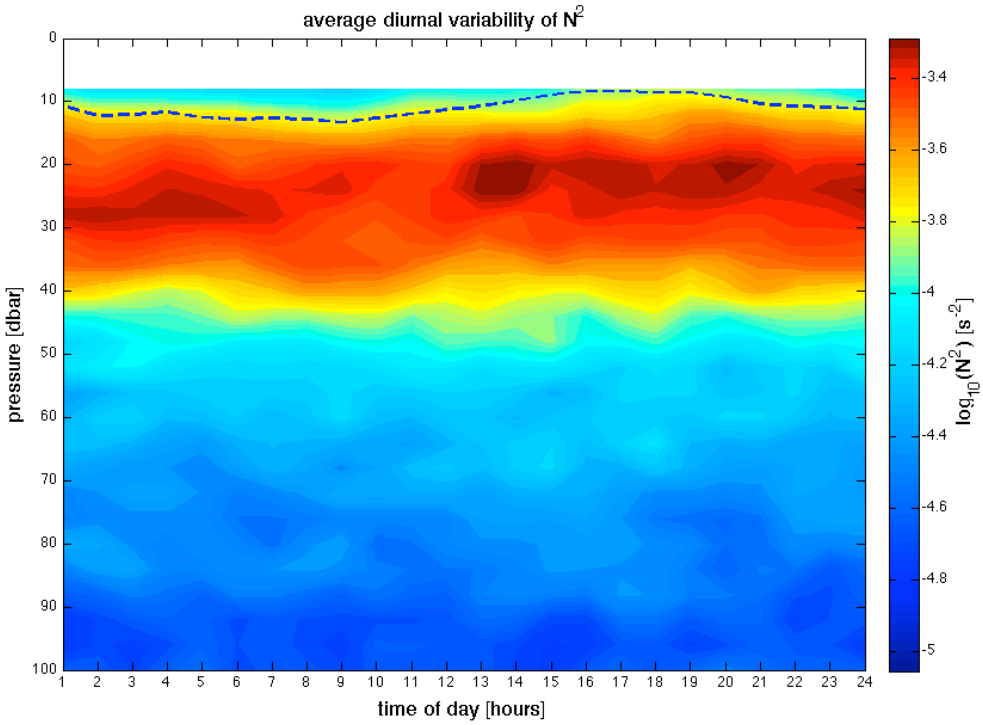

Figure 3-3: *average diurnal variability of the buoyancy-frequency N^2, mean profiles for each hour of the day derived from the data collected during the second deployment (06/13/11-06/29/11), blue dashed line: average mixed layer depth*

The total shear has been calculated by using binned data from ADCP measurements (figure 3-4). This limits the vertical resolution which can be reached when calculating the shear. Strong vertical shear is present down to 30 meters of depth throughout the whole day. The depth of increased levels of vertical shear shows a vague diurnal variability which might be due to tidal influences.

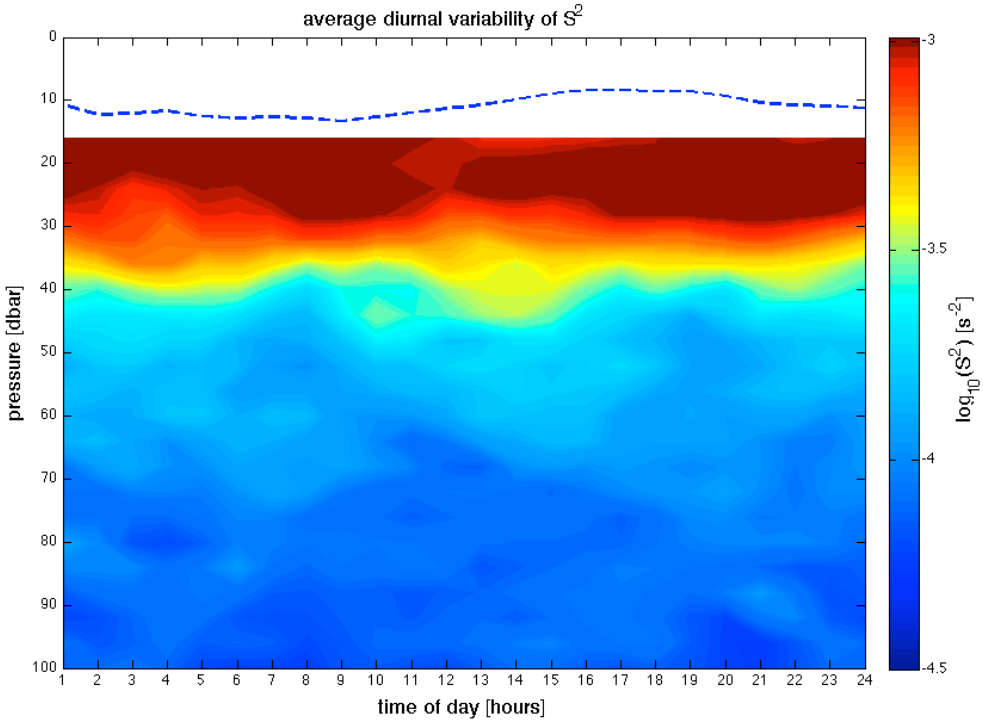

Figure 3-4: *average diurnal variability of the total shear S^2, mean profiles for each hour of the day derived from the data collected during the second deployment (06/13/11-06/29/11), blue dashed line: average mixed layer depth*

The Froude number indicates no distinct diurnal cycle (figure 3-5). The values nearest to the mixed layer depth would allow turbulent mixing most of the time. There is a slight decrease from 15:00 - 21:00 UTC and slightly increased values from 04:00 - 14:00 UTC. At about 30-40 meters below the surface a region of low Froude numbers can be found. The lowest values can be found from 06:00 - 11:00 UTC at 40 meters depth. In the layer below 40 meters of depth the Froude number reveals high values most of the time representing favorable conditions for turbulent mixing.

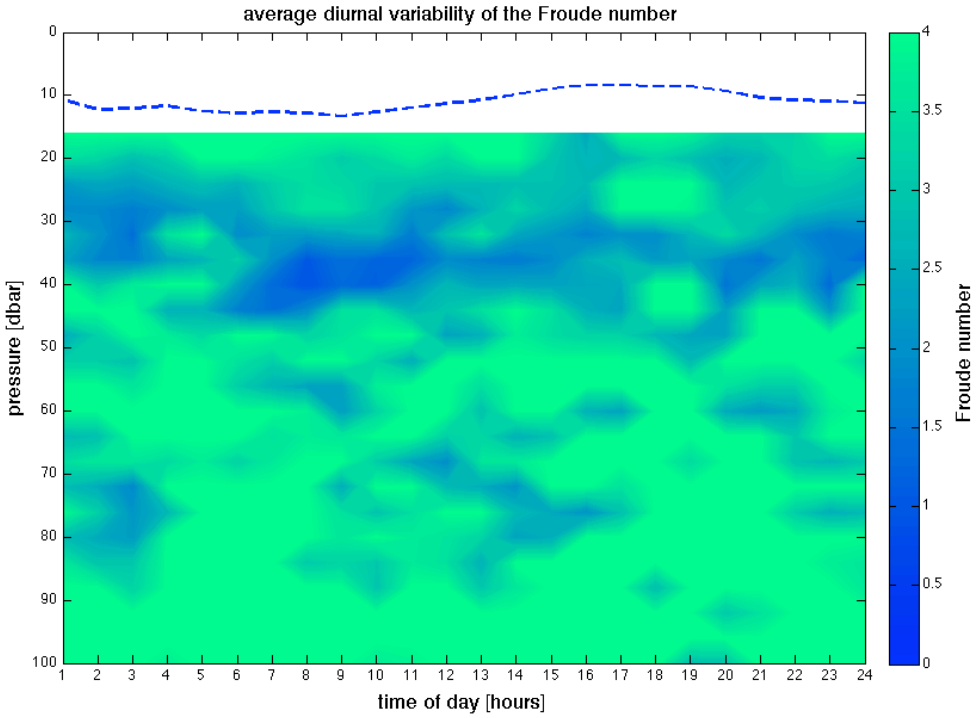

Figure 3-5: *average diurnal variability of the Froude number, mean profiles for each hour of the day derived from the data collected during the second deployment (06/13/11-06/29/11), blue dashed line: average mixed layer depth*

3.3 Vertical structure of the water column

Based on the diurnal cycle observed in section 3.2, a more thorough analysis of the vertical structure during several periods of the day has been performed.

The mixed layer is shallow during the afternoon when the solar radiation during the day warmed the upper layer (figure 3-6). The mixed layer depth from 08:00 - 14:00 UTC is the same as from 20:00 - 02:00 UTC. The mixed layer is deepest during the second half of the night. Elevated rates of turbulent kinetic energy dissipation rate can be observed in the surface mixed layer from 08:00 - 14:00 UTC. The lowest rates of ε in the surface mixed layer can be found during the night from 20:00 UTC to 08:00 UTC. Below the mixed layer depth the level of ε decreases rapidly during the day (08:00 - 20:00 UTC). The highest levels of ε below the mixed layer can be found during the second half of the night (02:00 - 08:00 UTC). Throughout that time, the

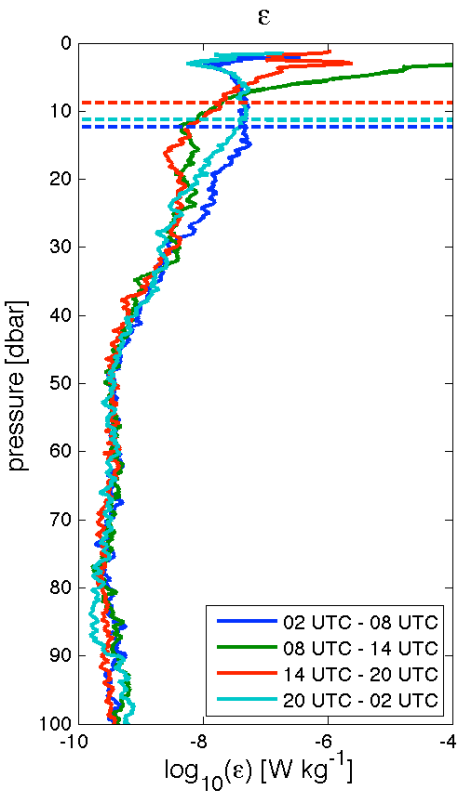

Figure 3-6: *vertical distribution of ε averaged for different times of the day, the dashed lines represent the respective averaged mixed layer depths*

levels of ε below the mixed layer have increased by a factor >10[1] compared to the period from 08:00 - 20:00 UTC. There is no noticeable decrease of ε at the mixed layer depth during the night, but constantly high rates of ε in a vertical extent of more than 10 meters. Below 30 meters of depth, no diurnal variability of ε can be distinguished.

The stratification shows a less distinct diurnal cycle (figure 3-7). There is a vertical stratification maximum at 20-30 meters of depth. Below 35 meters the stratification is constantly decreasing. The stratification at the mixed layer depth is highest during the second half of the day when the solar radiation has warmed the surface water masses and lowest during the second half of the night. Below the mixed layer depth the stratification is strongest during the second half of the day (14:00 - 20:00 UTC) and weakest from 02:00 - 08:00 UTC. Below 25 meters of depth, no distinct diurnal cycle has been noticed.

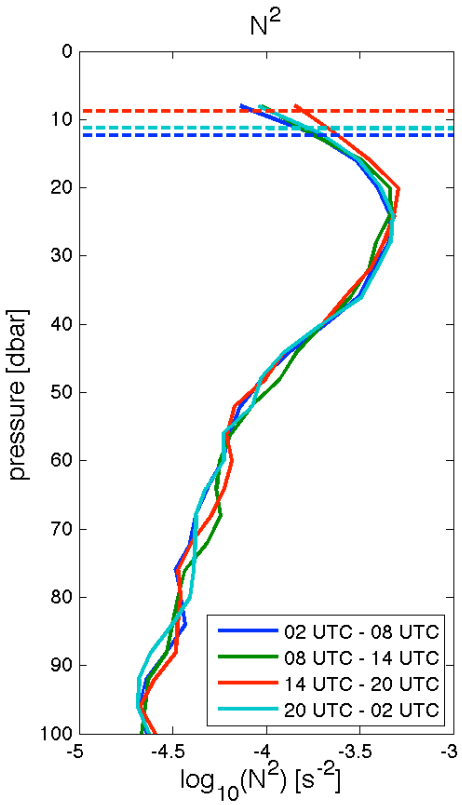

Figure 3-7: *vertical distribution of the stratification averaged for different times of the day, the dashed lines represent the respective averaged mixed layer depths*

The vertical shear has a maximum from 15 - 25 meters of depth (figure 3-8). The weakest shear in this layer has been observed during the first half of the day (08:00 - 14:00 UTC). The strongest shear is present at 20 meters depth from 20:00 - 02:00 UTC. Below this layer, the shear is constantly decreasing during the whole day. From 30 - 40 meters of depth, no distinct diurnal variation has been observed. The shear from 08:00 - 14:00 UTC is always weakest and from 02:00 - 08:00 UTC strongest but the variability is rather small.

A considerable increase of the shear has been observed at 45 meters depth during the first half of the day (08:00 - 14:00 UTC) while the shear at the same depth remains at a constant lower level during any other time of the day.

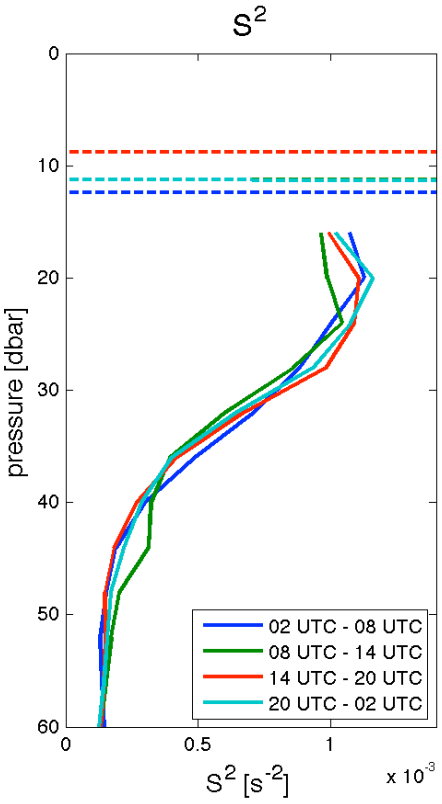

Figure 3-8: *vertical distribution of the shear averaged for different times of the day, the dashed lines represent the respective averaged mixed layer depths*

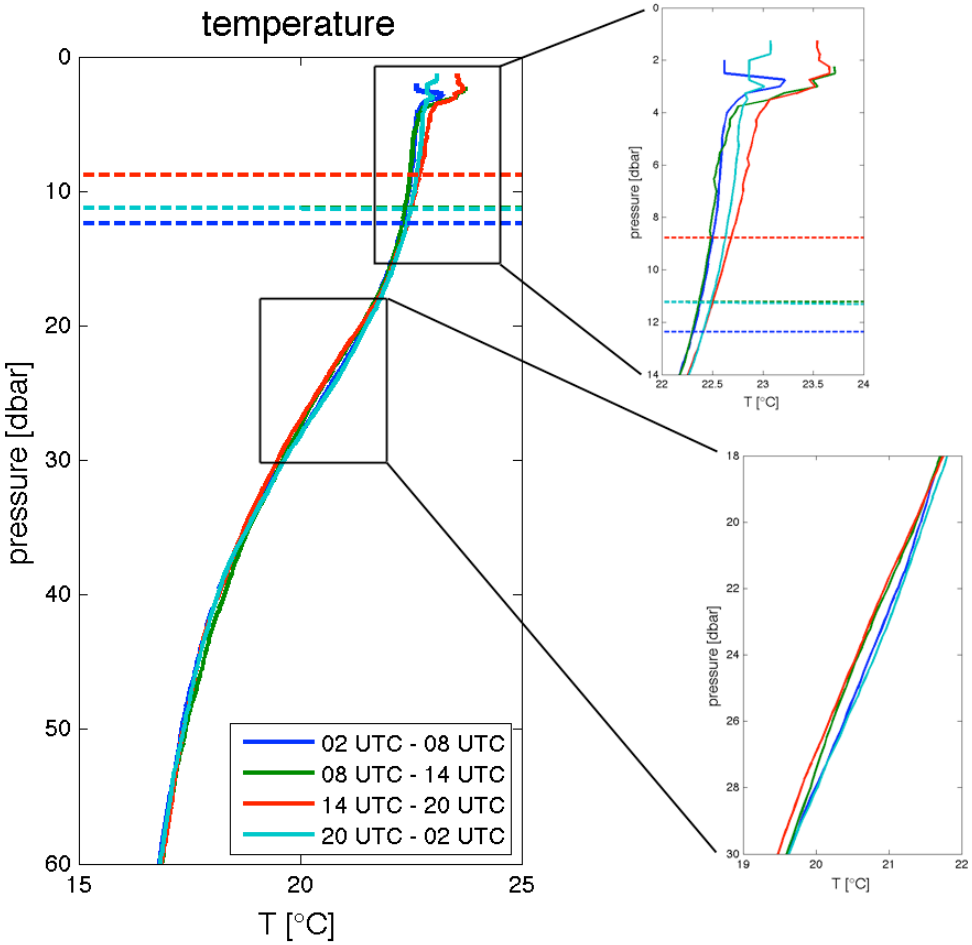

Figure 3-9: *vertical distribution of the temperature averaged for different times of the day, the dashed lines represent the respective averaged mixed layer depths*

The vertical distribution of the temperature during the day exhibits a strong diurnal cycle in the surface mixed layer (figure 3-9). A layer of 3 - 4 meters thickness at the surface is strongly affected by the solar heating during the day and cooling during the night. The highest temperature of 23.5 °C can be found near the surface after noon from 14:00 - 20:00 UTC. Below 4 meters of depth a diurnal cycle was present but the difference between the highest and lowest average temperature was never far above 0.5 °C. The highest temperature has been measured during the second half of the day, decreasing between 20:00 and 02:00 UTC until the minimum temperature of ~22.5 °C is reached and conserved until 14:00 UTC.

Below the mixed layer depth the temperature is decreasing without any obvious difference between daytime and nighttime values. Below 20 meters of depth a weak diurnal cycle has been observed. The observed average temperature from 22 - 28 meters of depth have been increased by about 0.3 °C during the night (20:00 - 08:00 UTC) compared to the temperatures measured during the day.

3.4 Spectral analysis

The presence of recurring mixing events below the mixed layer suggests that a spectral analysis of the data might reveal augmented levels of variability for some frequencies. Several time series at different constant depths and constant depths relative to the mixed layer depth have been analyzed.

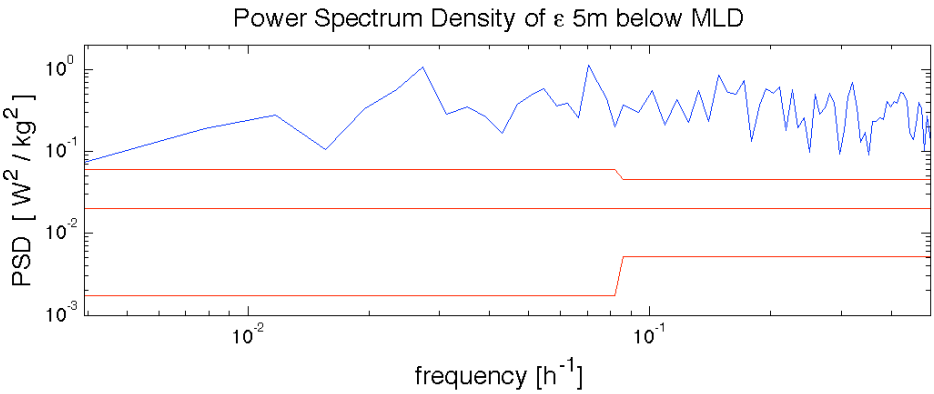

Figure 3-10: *Power Spectrum Density function of the time-series of ε 5 meters below the mixed layer, variance conserving, the red lines show the upper and lower 95% confidence boundary*

The Power Spectrum Density of the time series of ε 5 meters below the mixed layer shows high levels of variance for all frequencies (figure 3-10). Two broad peaks that are slightly above the 95% confidence boundary have been noticed. The associated periods are 35.7 hours and 14.3 hours. For periods below 10 hours there is high variance without any distinct peaks.

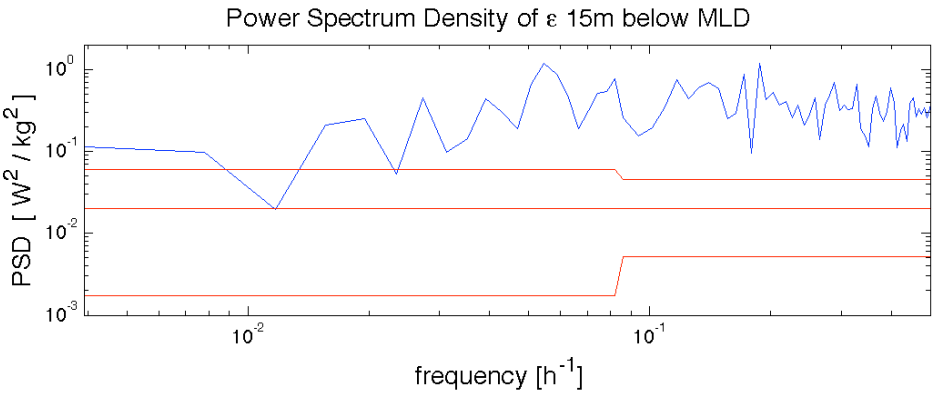

Figure 3-11: *Power Spectrum Density function of the time-series of ε 10 meters below the mixed layer, variance conserving, the red lines show the upper and lower 95% confidence boundary*

The time series of ε 15 meters below the mixed layer shows increased variance for a period of ~18 hours (figure 3-11). The variance for all periods below 10 hours is high whilst slightly decreasing towards shorter periods.

The calculated mixed layer depth changes more than 10 meters in less than a day (figure 3-1). Therefore periodic changes of the mixed layer depth might have a high influence on the spectral analysis. In order to avoid this influence, the Power Spectrum Density function of ε has been calculated for constant depths below the surface.

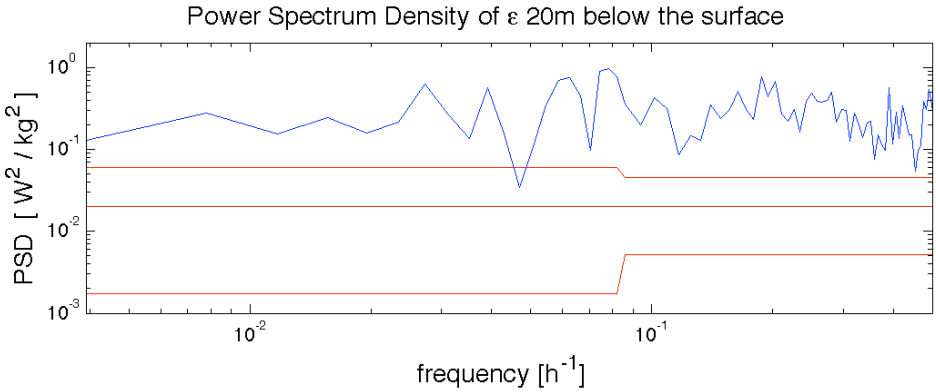

Figure 3-12: *Power Spectrum Density function of the time-series of ε 20 meters below the surface, variance conserving, the red lines show the upper and lower 95% confidence boundary*

The time series of ε 20 meters below the surface reveals increased variance between periods of 16.6 hours and 12.5 hours (figure 3-12). Increased variance can be observed for a period of 5 hours and for a period of 2.5 hours.

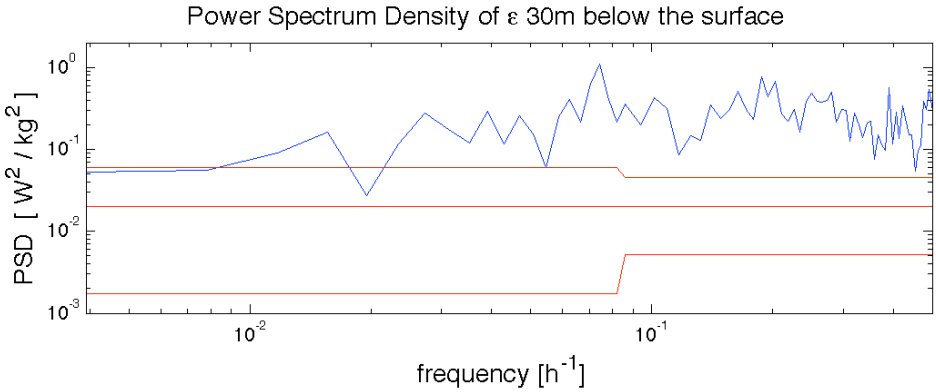

Figure 3-13: *Power Spectrum Density function of the time-series of ε 30 meters below the surface, variance conserving, the red lines show the upper and lower 95% confidence boundary*

The time series of ε 30 meters below the surface (figure 3-13) reveals increased variance similar to the time series 20 meters below the surface. There is a more distinct peak at a period of 13.7 hours. Similar to figure 3-12, the variance is higher near periods of 5 hours and 2.5 hours.

In addition to the spectral analysis of ε, the time series of the vertical shear have been analyzed for frequencies with increased variance.

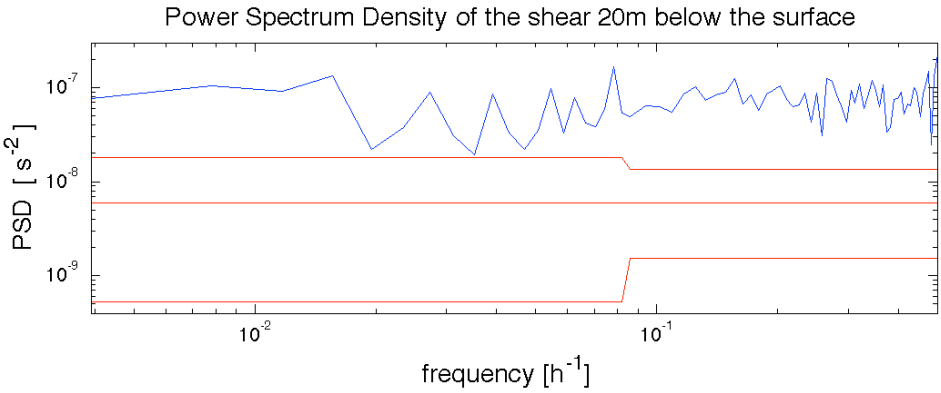

Figure 3-14: *Power Spectrum Density function of the time-series of the shear 20 meters below the surface, variance conserving, the red lines show the upper and lower 95% confidence boundary*

The shear 20 meters below the surface has an increased variance on periods longer than 70 hours (figure 3-14). A distinct peak slightly above the 95% confidence boundary is present for a period of 12.5 hours.

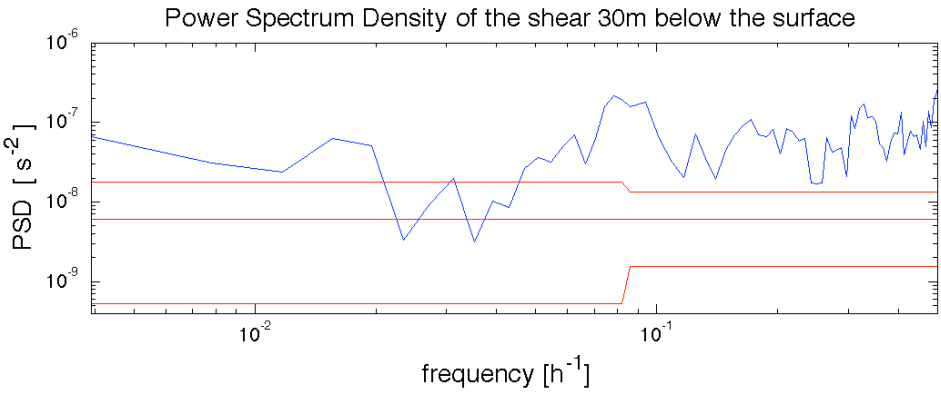

Figure 3-15: *Power Spectrum Density function of the time-series of the shear 30 meters below the surface, variance conserving, the red lines show the upper and lower 95% confidence boundary*

Increased variance well above the 95% confidence boundary can be found for periods between 13 hours and 10 hours in the time series of the shear 30 meters below the surface (figure 3-15). For most periods below 10 hours the variance is high. The most conspicuous peak can be found for periods slightly below 2.5 hours.

4 Discussion

4.1 Interpretation

Two prominent cycles have been found by analyzing the glider measurements. There is a diurnal cycle of enhanced turbulent mixing below the mixed layer depth with a maximum during the second half of the night until noon of the next day. The diurnal cycle is superimposed on a low frequent cycle with a period of 11 days. This low frequent variability is followed by an increased vertical extent and an increased rate of mixing in the thermocline around the 15th and 26th of June. In between these maxima, on the 19th of June, no turbulent mixing was recorded in the thermocline. The vertical extent and intensity of mixing events reveal a distinct interconnection with high Froude numbers. The most likely explanation for the low-frequent variability is the passing of a tropical instability wave which induces an increased shear and thus pushes the flow towards instability (Moum et al. 2009).
The intensification of turbulent mixing on a diurnal basis is always connected to high Froude numbers. However, in reverse there have been favorable conditions for turbulent mixing when no turbulent mixing occurred. This suggests a mechanism that triggers turbulent mixing. Moum et al. came to the conclusion that ε can not be predicted from the Froude number alone, mixing also depends on other forcings not expressed by the Froude number (Moum et al. 1989).
The deep diurnal cycle seems to have an impact on the temperature below the mixed layer. During the night, an increase of about 0.3 °C has been noticed in the depth range of 20 - 30 meters. The temperature is slightly higher before mixing occurs (before 02:00 UTC). This suggests that the increased temperature is not a result of the mixing but might rather be connected to the circumstances that lead to mixing. Below 50 meters of depth another layer of enhanced mixing activity can be found. This layer is characterized by high Froude numbers but has no apparent connection to the mixing regime in the thermocline. A similar regime, found in the equatorial Pacific (Moum et al. 2009), has been attributed to three-dimensional processes that have not been resolved in the measurements.
The spectral analysis of ε reveals high levels of variance of all frequencies. The diurnal cycle is not visible as an increase in variance. The increased shear variance 30 meters below the surface with a period of about 12 hours might be linked to tidal influences.
The character of the mixing events in the thermocline as previously observed (Moum et al. 1989) can lead to difficulties in locating the events with the methods used in this study. Short bursts of enhanced rates of ε that last 2-3 hours and do not occur at the same time

each day lead to an imprecise detection when calculating mean values for specific periods. This implies that the actual mixing events might have been stronger than the results suggest. The outcome of the spectral analysis suffers from the non-uniformly spaced measurements as well as from a varying length of the intervals between two mixing events.

The data provided for this study offer a unique perspective for understanding the processes below the mixed layer in the equatorial Atlantic. The simultaneous measurement of current velocities and turbulent mixing processes provides substantial information on the interconnection between different mechanisms in the water column.

As the glider based measurement of turbulent kinetic energy dissipation rate has just recently become possible, there are not many well-established methods for treating such data. The glider profiles the water column with a vertical velocity of 0.14 ms^{-1}. At this rate the glider needs 83 minutes to dive down to a depth of 350 meters and return to the surface. For the time in between two measurements no in situ data is available. This produces an uncertainty of the exact duration of mixing events. The data has been interpolated on a grid with each profile assigned to a specific time. As the properties of the diurnal cycle in the tropical Atlantic are not yet fully explored, the interpolation bears the possibility of interfering with some signals in the recorded data that might belong to mechanisms that have not yet been fully understood.

This study has revealed a diurnal cycle of mixing events below the surface mixed layer in the equatorial Atlantic similar to former studies in the equatorial Pacific (Moum et al. 1992).

4.2 Perspectives

Vertical mixing in the Equatorial Atlantic is supposed to be a key mechanism in the development of the Atlantic Cold Tongue (Giordani 2011).Therefore it is essential to know the driving forces of these mixing processes and their regional and temporal variability to be able to simulate the development of the Atlantic Cold Tongue and include these processes into future models.

In this study, the influence of solar radiation and wind intensity at the surface have been neglected as well as the influence of other currents than the EUC. The two-dimensional approach (vertical and temporal distribution) employed in this study allows a thorough investigation of the deep diurnal cycle. The current shear has been found to have a significant influence on the diurnal cycle but beyond these findings, it is difficult to analyze the mechanisms that drive the diurnal cycle. A more-dimensional approach will be inevitable to fully understand these features.

The equatorial current system is highly complex. It is therefore difficult to examine the influence of a specific current, while neglecting the influence of other currents and features such as tropical instability waves. The equatorial current system is closely connected with atmospheric forcing. Additional data for wind stress and radiative forcing should be taken into account. The PIRATA network provides this information from several moored buoys in the equatorial Atlantic.

Shipboard ADCP measurements and CTD casts collected in the equatorial Atlantic region might provide a hint to whether the conditions have been favorable for turbulent mixing processes below the mixed layer depth at other times.

It is of central importance to find the mechanism that drives the deep diurnal cycle. Only thereafter it will be possible to implement this process into models and to simulate the variability of diapycnal mixing accurately.

References

Dengler, M. (1995): *Entstehung von homogenen Schichten durch äquatoriale Wellen*. *Diplomarbeit*.

Giordani, H. (2011): Diagnosing vertical motion in the Equatorial Atlantic. *Ocean Dynamics*, **61**, 1995–2018.

Gregg, M., H. Peters, J. Wesson, N. Oakey, and T. Shay (1985): Intensive measurements of turbulence and shear in the equatorial undercurrent. *Nature*, **318**, 140–144.

Hebert, D., J. Moum, C. Paulson, and D. Caldwell (1992): Turbulence and internal waves at the equator. II: Details of a single event. *J Phys Oceanogr*, **22**, 1346–1356.

Jouanno, J., F. Marin, Y. du Penhoat, J. M. Molines, and J. Sheinbaum (2011): Seasonal Modes of Surface Cooling in the Gulf of Guinea. *J Phys Oceanogr*, **41**, 1408–1416, doi:10.1175/JPO-D-11-031.1.

Lien, R. C., D. R. Caldwell, M. Gregg, and J. N. Moum (1995): Turbulence variability at the equator in the central Pacific at the beginning of the 1991-1993 El Niño. *J. Geophys. Res.*, **100**, 6881-6898.

MCPHADEN, M. J., and H. Peters (1992): Diurnal cycle of internal wave variability in the equatorial Pacific Ocean: results form moored observations. *J Phys Oceanogr*, **22**, 1317–1329.

Moum, J. N., D. R. Caldwell, and C. A. Paulson (1989): Mixing in the equatorial surface layer and thermocline. *J. Geophys. Res*, **94**, 2005–2021.

Moum, J. N., R. C. Lien, A. Perlin, J. D. Nash, M. C. Gregg, and P. J. Wiles (2009): Sea surface cooling at the Equator by subsurface mixing in tropical instability waves. *Nature Geoscience*, **2**, 761–765, doi:10.1038/ngeo657.

Moum, J., M. McPhaden, D. Hebert, H. Peters, C. Paulson, and D. Caldwell, (1992): Internal waves, dynamic instabilities, and turbulence in the equatorial thermocline: An introduction to three papers in this issue. *J Phys Oceanogr*, **22**, 1357–1360.

Pedlosky, J. (1996): Ocean circulation theory (1996, corr. 2nd printing 1998).

Peters, H., M. Gregg, and J. Toole (1988): On the parameterization of equatorial turbulence. *J. Geophys. Res*, **93**, 1199–1218.

Richards, K. J., Y. Kashino, A. Natarov, and E. Firing (2012): Mixing in the western equatorial Pacific and its modulation by ENSO. *Geophys. Res. Lett*, **39**, doi:10.1029/2011GL050439.

Thorpe, S. A. (1973): Turbulence in stably stratified fluids: A review of laboratory experiments. *Boundary-Layer Meteorol*, **5**, 95–119, doi:10.1007/BF02188314.

Acknowledgements

I would like to express my gratitude to my supervisor Dr. Marcus Dengler for his support and guidance in this study as well as for the suggestion of the interesting topic.

I want to thank everyone who has been involved in the processing of the data from the glider missions. Furthermore, I want to thank the TAO Project Office for providing data from the Prediction and Research Moored Array in the Tropical Atlantic (PIRATA) and Remote Sensing Systems for providing satellite measurements of the sea surface temperature.

Finally I would like to thank my parents for their support of my studies.

Statement / Erklärung

I hereby declare that I have written the Bachelors Thesis on my own and have used no other than the stated sources and aids. The submitted written version is equivalent to the electronical data medium. Furthermore, I affirm that this work has not been submitted for any other degree.

Hiermit erkläre ich, dass ich die vorliegende Arbeit selbstständig und ohne fremde Hilfe angefertigt und keine anderen als die angegebenen Quellen und Hilfsmittel verwendet habe. Die eingereichte schriftliche Fassung der Arbeit entspricht der auf dem elektronischen Speichermedium. Weiterhin versichere ich, dass diese Arbeit noch nicht als Abschlussarbeit an anderer Stelle vorgelegen hat.

_____ Ort, Datum Unterschrift